

Accepted Manuscript

Design, synthesis and bioevaluation of 1,2,3,9-tetrahydropyrrolo[2,1-*b*]quinazoline-1-carboxylic acid derivatives as potent neuroprotective agents

Linkui Zhang, Ying Zhao, Jian Wang, Donglin Yang, Chenwen Zhao, Changli Wang, Chao Ma, Maosheng Cheng



PII: S0223-5234(18)30294-0

DOI: [10.1016/j.ejmech.2018.03.052](https://doi.org/10.1016/j.ejmech.2018.03.052)

Reference: EJMECH 10317

To appear in: *European Journal of Medicinal Chemistry*

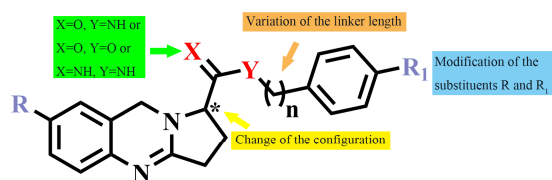
Received Date: 18 January 2018

Revised Date: 16 March 2018

Accepted Date: 17 March 2018

Please cite this article as: L. Zhang, Y. Zhao, J. Wang, D. Yang, C. Zhao, C. Wang, C. Ma, M. Cheng, Design, synthesis and bioevaluation of 1,2,3,9-tetrahydropyrrolo[2,1-*b*]quinazoline-1-carboxylic acid derivatives as potent neuroprotective agents, *European Journal of Medicinal Chemistry* (2018), doi: 10.1016/j.ejmech.2018.03.052.

This is a PDF file of an unedited manuscript that has been accepted for publication. As a service to our customers we are providing this early version of the manuscript. The manuscript will undergo copyediting, typesetting, and review of the resulting proof before it is published in its final form. Please note that during the production process errors may be discovered which could affect the content, and all legal disclaimers that apply to the journal pertain.



- ▶ Synthesis, SAR
- ▶ Ca²⁺ influx, Western-blot, computer docking studies
- ▶ In vitro metabolic stability study

ACCEPTED MANUSCRIPT

Design, synthesis and bioevaluation of 1,2,3,9-tetrahydropyrrolo[2,1-*b*]quinazoline-1-carboxylic acid derivatives as potent neuroprotective agents

Linkui Zhang ^a, Ying Zhao ^a, Jian Wang ^a, Donglin Yang ^a, Chenwen Zhao ^a, Changli Wang ^b, Chao Ma ^{a,*}, Maosheng Cheng ^{a,*}

^a *Key Laboratory of Structure-Based Drug Design & Discovery of Ministry of Education, School of Pharmaceutical Engineering, Shenyang Pharmaceutical University, 103 Wenhua Road, Shenhe District, Shenyang 110016, PR China*

^b *Department of Pharmacy, General Hospital of Shenyang Military Area Command, 83 Wenhua Road, Shenhe District, Shenyang 110840, PR China*

* Email address: machao_syphu@163.com (C. Ma); mscheng@syphu.edu.cn (M. Cheng)

Abstract

Diverse of 1,2,3,9-tetrahydropyrrolo[2,1-*b*]quinazoline-1-carboxylic acid derivatives were designed, synthesized and evaluated for their neuroprotective activity against NMDA-induced cytotoxicity in vitro, and **5q** exhibited excellent neuroprotective activity. The compound **5q** was selected for further investigation. We found that **5q** could attenuate Ca²⁺ influx induced by NMDA, meanwhile, **5q** could suppress the NR2B up-regulation and increase p-ERK1/2 expression. The molecular docking results showed that **5q** might fit well in the binding pocket of **4** and interact with some key residues in the binding pocket of **1** simultaneously. Besides, **5q** exhibited acceptable metabolic stability. These results suggested that **5q** was a promising lead for further development of new potent and orally bioavailable NR2B-selective NMDAR antagonists.

Key words: Neuroprotective activity, Ca²⁺ influx, p-ERK1/2, NR2B-selective NMDAR antagonists

1. Introduction

Glutamate is the principal excitatory neurotransmitter in the central nervous system

(CNS), which mediates its effects via activation of metabotropic glutamate (mGlu) and ionotropic glutamate (iGlu) receptors [1, 2], while glutamate accumulation and excessive stimulation of its receptors induce potent excitotoxicity in the CNS [3]. The *N*-methyl-D-aspartate receptors (NMDARs) belong to the family of iGlu receptors [4], which play a pivotal role in mediating glutamate excitotoxicity [5]. Overactivation of NMDARs can lead to Ca^{2+} overload of neurons, which is associated with a number of acute and chronic neurodegenerative diseases, including stroke, seizures, Parkinson's disease, and chronic pain [6-8]. NMDARs are heterotetrameric proteins, consisting of three types of subunits: NR1 (NR1a-h), NR2 (NR2A-D), and NR3 (NR3A-B) [9]. A functional NMDAR protein contains at least one NR1 subunit and one NR2 subunit [10], indeed, excitotoxicity is triggered by the selective activation of NMDARs containing the NR2B subunits [11]. The ERK signaling pathway is activated by calcium influx through NMDARs and plays an important role in synaptic plasticity and cell survival [12, 13]. It has been proposed that NR2B-containing NMDARs are mainly involved in the inhibition of ERK1/2 activity [14, 15].

The neuroprotective potential of NR2B-selective NMDAR antagonists can be exploited for the treatment of neurodegenerative diseases like stroke, Alzheimer's disease and Parkinson's disease. Compared to non-subtype selective NMDA receptor antagonists, NR2B selective antagonists might have less side effects [16]. **1** (ifenprodil) [17] was the first reported NR2B-selective NMDAR antagonist (**Figure 1**), unfortunately, its selectivity is poor. The interaction of **1** with other receptors (α_1 , σ_1 , σ_2 , 5-HT_{2A} and 5-HT_{2C} receptor), leads to undesired side effects, e.g. impaired motor function. Besides, the bioavailability of **1** is rather low due to its fast biotransformation [18]. Nevertheless, **1** serves as an important lead structure for the rational design of novel NR2B-selective NMDAR antagonists, such as **2** (traxoprodil, CP-101,606) [19]. Research efforts have focused on identifying novel structural classes of NR2B-selective NMDAR antagonists for improving the potency, selectivity profiles and the metabolic stability, for example, **3** is a potent orally bioavailable, NR2B-selective NMDAR antagonist with antidepressant effects [20]. In 2016, David Stroebel et al. reported the crystal structure of the NR1/NR2B heterodimer in complex

with **4** [21], the binding site of **4** revealed a remarkably different situation with a shared interdomain cavity but little overlap with the binding site of **1**. These data widen the allosteric and pharmacological landscape of NMDARs and facilitate the design of NR2B-selective NMDAR antagonists with therapeutic value for brain disorders.

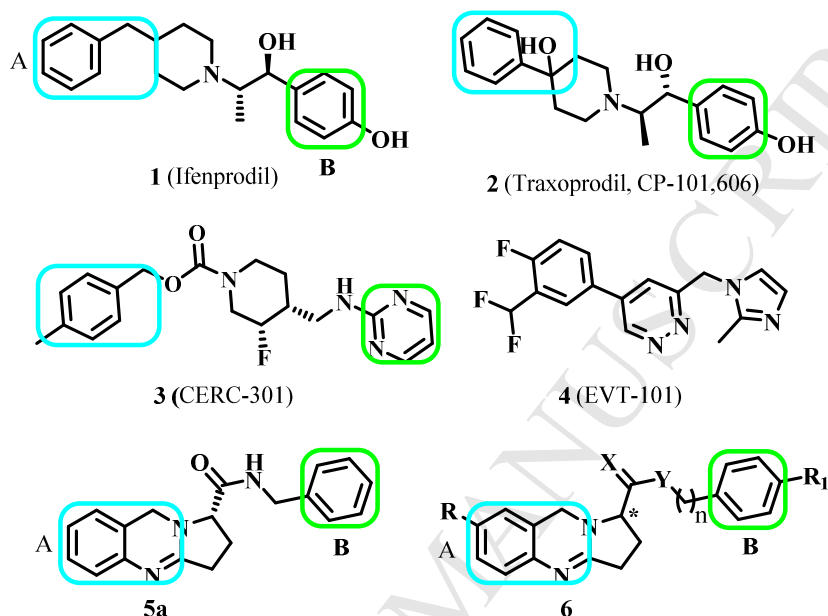


Figure 1. Chemical structures of several representative NR2B-selective NMDAR antagonists (**1-4**), *S*-1,2,3,9-tetrahydropyrrolo[2,1-*b*]quinazoline-1-carboxylic acid derivative (**5a**) and general structure (**6**) of designed compounds.

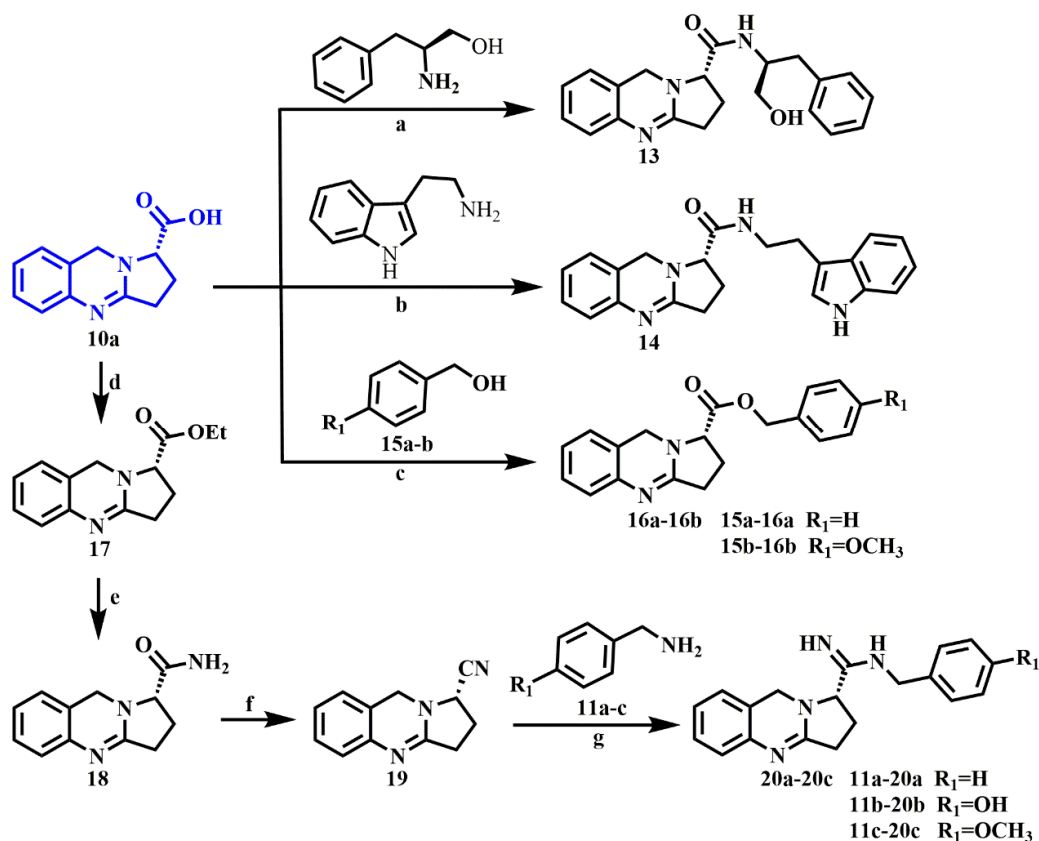
A previous study had found that **5a** (**Figure 2**) could protect against ischemia-induced cell injury in an oxygen glucose deprivation (OGD) model of ischemic stroke [22]. We noted that the structure of compound **5a** contains the similar features with many NR2B-selective NMDAR antagonists (e.g. **1-3**): one hydrophobic aromatic part (**A**) links to another aromatic part (**B**). Inspired by the neuroprotective activity and the outstanding structure of **5a**, we attempted to search for potent neuroprotective agents with the hope of identifying structurally distinct NR2B-selective NMDAR antagonists. In this study, a series of 1,2,3,9-tetrahydropyrrolo[2,1-*b*]quinazoline-1-carboxylic acid derivatives (**6**) were designed, synthesized and evaluated for the neuroprotective activity, and **5q** was identified as an effective neuroprotective agent in vitro NMDA-induced cytotoxicity model. We assume that NR2B-NMDARs were involved in the neuroprotection of **5q**.

To verify the hypothesis, the compound **5q** was selected for further investigation. First, we measured the intracellular calcium concentration change caused by *N*-methyl-D-aspartate (NMDA) pretreatment with or without **5q** using the laser scanning confocal microscope. Then the potential effects of **5q** on NMDA-induced apoptosis were verified by western-blot assay. Finally, computational molecular docking methods were used to predict the potential molecular interaction mechanisms between **5q** and NR2B-NMDARs. Besides, we evaluated the in vitro metabolic stability of **5q**.

2. Results and discussion

2.1. Chemistry

The key intermediates **10a-10d** were synthesized through the method described previously [26] (**Scheme 1**). The reductive amination of **7a-7b** using L- or D-glutamic acid gave the intermediates **8a-8d**. The subsequent intramolecular cyclization and dehydration in refluxing ethanol produced the intermediates **9a-9d**. Finally, compounds **9a-9d** were treated with 80% hydrazine hydrate, $\text{FeCl}_3 \cdot 6\text{H}_2\text{O}$, and activated carbon in refluxing ethanol for 3 days, yielding the key intermediates **10a-10d**. The target compounds **5a-5s** and **12a-12j** were prepared via the amidation of intermediates **10a-10d** with **11a-11m**. The similar method was used to synthesize the compounds **13**, **14** and **16a-16c** (**Scheme 2**).



Scheme 2. Reagents and conditions: (a) BOP-Cl, Et₃N, 0 °C~r.t., 6 h; (b) BOP-Cl, Et₃N, 0 °C~r.t., 6 h; (c) BOP-Cl, Et₃N, 0 °C~r.t., 6 h; (d) SOCl₂, CH₃CH₂OH, -5 °C~r.t., 6 h; (e) Aqueous solution of ammonia, 50 °C, 3 h; (f) POCl₃, DMF, 50 °C, 4 h; (g) i, CH₃CH₂OH, HCl (g); ii, Et₃N, CH₃CH₂OH.

2.2. Biological evaluation

All of the synthesized compounds were evaluated for their neuroprotective effects on SH-SY5Y cells damaged by NMDA via 3-(4,5-Dimethylthiazol-2-yl)-2,5-diphenyl-tetrazolium bromide (MTT) assay. The results were presented in **Table 1** and **Table 2**.

Based on the *in vitro* neuroprotective activities shown in **Table 1**, it was observed that the *S*-1,2,3,9-tetrahydropyrrolo[2,1-*b*]quinazoline-1-carboxylic acid amides derivatives were considerably more effective than the corresponding esters and amidines derivatives (**5a-5c** versus **16a-16b**, **20a-20c**). The neuroprotection of **5a-5e** were similar to each other, which suggested that R_1 could be some small substituent groups, such as methyl, hydroxyl and halogen. In consideration of increasing the metabolic stability, we introduced the substituent Br to the benzene ring of part **A**, this

modification did not have major influences on the activity (**5b-5e** versus **5f-5h**).

At low to moderate concentration (0.1, 1, 10 μ M), almost all of the compounds **5m-5q** (n=2) exhibited more potent neuroprotection than **5a-5h** (n=1), **5i-5l** (n=0) and **5r-5s** (n=3), so it is obvious that the distance between the acylamino and the benzene ring of part **B** played a crucial role in the neuroprotection of the compounds, and the optimal length of the alkyl spacer was 2 methylene moieties, shorting or lengthening the length of alkyl spacer would reduce the activity. Among these compounds, the compound **5q** (75.8%, 80.0%, 84.4%, 78.6%) exhibited slightly higher potency than ifenprodil (71.0%, 72.7%, 79.5%, 65.1%) at the test concentration.

Given the compounds had a chiral center, a few *R*-1,2,3,9-tetrahydropyrrolo[2,1-*b*]quinazoline-1-carboxylic acid derivatives (**12a-12j**) were synthesized and evaluated for their neuroprotective activity. Although almost all of the *R*-derivatives were less active than their *S*-configuration counterparts, the differences in potency were small (**Table 2**). Therefore, in spite of the *S*-configuration was a little better for these derivatives, the chiral center did not affect the neuroprotective potency significantly. To extend the investigation range, we introduced a hydroxymethyl substituent into the methylene of **5m** or replaced the benzene ring by indole ring, and the compounds **13** and **14** were synthesized according to the synthetic routes shown in **Scheme 2**, both of their neuroprotective potency were comparable to **5m**.

Table 1. The influences of target compounds on NMDA-damaged SH-SY5Y cells

Compd.	Cell viability ^a (%)			
	0.1 μ M	1 μ M	10 μ M	100 μ M
Control	100 ^b			
Model	58.7 ^c \pm 2.3			
5a	68.4 ^f \pm 2.5	71.6 ^f \pm 0.6	70.5 ^f \pm 2.9	64.4 ^e \pm 1.0
5b	67.6 ^f \pm 0.6	72.0 ^f \pm 1.6	73.8 ^f \pm 1.3	70.3 ^f \pm 1.8
5c	68.1 ^f \pm 1.0	71.8 ^f \pm 2.7	74.1 ^f \pm 0.3	64.4 ^e \pm 2.2
5d	67.1 ^e \pm 3.5	72.6 ^f \pm 0.5	78.9 ^f \pm 3.3	63.2 \pm 1.7
5e	66.2 ^e \pm 3.2	73.4 ^f \pm 2.7	72.5 ^f \pm 2.9	54.5 \pm 2.2
5f	69.0 ^f \pm 1.4	73.5 ^f \pm 0.1	76.0 ^f \pm 3.2	60.0 \pm 0.4

5g	60.4±0.6	68.8 ^d ±3.1	74.3 ^e ±7.0	55.3±4.6
5h	64.8 ^f ±0.5	70.4 ^f ±1.6	70.4 ^f ±0.7	60.1±1.3
5i	68.7 ^f ±2.6	71.4 ^f ±2.3	60.4±1.7	54.6±1.4
5j	67.7 ^e ±2.8	68.3 ^e ±2.9	70.1 ^f ±2.8	70.9 ^f ±2.9
5k	64.7±1.9	72.7 ^f ±0.4	66.4 ^d ±5.9	48.4 ^d ±2.0
5l	62.9 ^e ±2.3	66.2 ^f ±0.2	68.0 ^f ±0.8	68.4 ^f ±0.8
5m	73.7 ^f ±1.3	77.6 ^f ±4.2	80.0 ^f ±0.2	57.5±0.4
5n	67.7 ^f ±0.4	78.1 ^f ±3.0	81.4 ^f ±1.2	67.8 ^f ±2.2
5o	73.0 ^f ±2.7	81.0 ^f ±3.4	75.1 ^f ±2.7	60.0±1.1
5p	71.4 ^f ±1.6	75.4 ^f ±4.0	68.1 ^e ±2.3	33.5 ^f ±1.0
5q	75.8 ^f ±0.8	80.0 ^f ±4.5	84.4 ^f ±4.0	78.6 ^f ±0.8
5r	67.2 ^f ±1.3	71.2 ^f ±0.6	63.4 ^e ±2.1	30.3 ^f ±2.6
5s	69.1 ^f ±2.1	76.6 ^f ±0.9	66.1 ^f ±0.4	42.2 ^f ±2.2
16a	61.0 ^d ±0.1	65.5 ^f ±0.9	66.1 ^f ±1.9	57.4±0.3
16b	61.4 ^d ±0.7	64.1 ^f ±1.2	65.3 ^f ±1.1	63.6 ^e ±1.8
20a	61.6±0.3	68.6 ^f ±4.0	68.8 ^f ±1.5	66.4 ^f ±1.8
20b	61.6±1.7	69.2 ^f ±1.5	70.2 ^f ±3.0	64.3 ^e ±0.4
20c	64.8 ^f ±1.7	65.8 ^f ±0.5	66.1 ^f ±1.0	56.9±1.8
1	71.0 ^f ±3.0	72.7 ^f ±0.4	79.5 ^f ±1.0	65.1 ^e ±1.6

^a Cell viability was calculated from the results, data are presented as the mean ± SD of three independent experiments.

^b The survival rates of Control group were 100%.

^c The survival rates of Model group treated by NMDA (2 mM) alone.

Statistical significance comparison was determined by one-way ANOVA. Compared with Model group: ^d p < 0.05. ^e p < 0.01. ^f p < 0.001.

Table 2. The influences of target compounds on NMDA-damaged SH-SY5Y cells

Compd.	Cell viability ^a (%)			
	0.1µM	1µM	10µM	100µM
Control	100 ^b			
Model	58.7 ^c ±2.3			
12a	65.2 ^e ±1.6	68.0 ^f ±3.0	64.2 ^e ±0.6	60.9±0.9
12b	66.6 ^f ±1.0	70.7 ^f ±2.6	76.2 ^f ±2.1	58.4±0.8
12c	71.1 ^f ±3.2	74.7 ^f ±3.5	72.9 ^f ±2.1	63.9 ^d ±1.2

12d	75.0 ^f ±4.6	78.0 ^f ±2.2	67.4 ^d ±3.8	56.9±4.1
12e	65.6 ^f ±2.1	67.2 ^f ±1.0	69.6 ^f ±1.6	73.3 ^f ±0.6
12f	61.7±3.4	71.3 ^f ±2.3	68.3 ^f ±0.6	66.0 ^e ±0.7
12g	65.2 ^d ±0.7	80.7 ^f ±3.6	70.5 ^f ±4.0	68.0 ^e ±0.8
12h	67.8 ^f ±1.1	74.5 ^f ±3.5	78.2 ^f ±1.2	81.5 ^f ±0.7
12i	62.2 ^d ±0.5	71.6 ^f ±2.5	70.2 ^f ±2.9	42.0 ^f ±0.3
12j	58.1±1.6	72.1 ^f ±3.8	65.4 ^d ±4.1	44.1 ^e ±0.7
13	67.1 ^e ±2.6	82.6 ^f ±2.5	79.6 ^f ±1.9	72.4 ^f ±3.9
14	66.2 ^d ±0.8	72.0 ^f ±4.6	80.9 ^f ±3.0	78.2 ^f ±1.7

^a Cell viability was calculated from the results, data are presented as the mean ± SD of three independent experiments.

^b The survival rates of Control group were 100%.

^c The survival rates of Model group treated by NMDA (2 mM) alone.

Statistical significance comparison was determined by one-way ANOVA. Compared with Model group: ^d p < 0.05. ^e p < 0.01. ^f p < 0.001.

2.3. Effect of **5q** on NMDA-induced Ca²⁺ influx in SH-SY5Y cells

Overactivation of NMDARs can lead to Ca²⁺ overload of neurons. Ca²⁺ is a key mediator of excitotoxic damage, which can activate a number of Ca²⁺-dependent enzymes and influence a multitude of cellular processes [23]. Overactivation of the NMDARs induced massive influx of Ca²⁺ into the neuron, the interaction of NR2B-selective NMDAR antagonists with the NMDARs could inhibit the influx of Ca²⁺. In this study, we evaluated the effects of **5q** on calcium influx (**Figure 3**). The results showed that compared with the control group, the intracellular Ca²⁺ increased markedly after NMDA was added, while the Ca²⁺ influx could be attenuated significantly when the SH-SY5Y cells were pretreated with **5q**. So, **5q** could inhibit the influx of Ca²⁺ induced by NMDA.

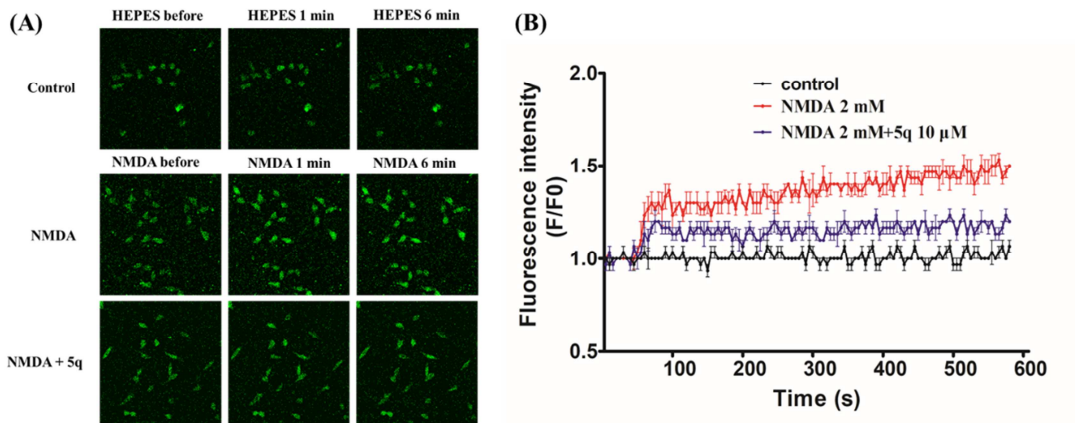


Figure 2. Calcium imaging of NMDA-induced Ca^{2+} influx. SH-SY5Y cells were loaded with fluo-3, the fluorescence intensity represents cytoplasmic Ca^{2+} concentration. (A) The green fluorescence under laser scanning microscope at different times showed the intracellular Ca^{2+} concentration in SH-SY5Y cells. (B) Fluorescence intensity of the control group during detection time. The fluorescence intensity showed that the intracellular Ca^{2+} concentration was stable in control group during detection time ($n = 9$ cells), NMDA (final concentration was 2 mM) was able to evoke Ca^{2+} influx markedly ($n = 9$ cells), while the Ca^{2+} influx could be attenuated significantly when the SH-SY5Y cells were pretreated with **5q** ($n = 9$ cells).

2.4. Effects of **5q** on the NR2B and the phosphorylated ERK1/2 (p-ERK1/2) expression

NR2B-containing NMDARs directly link NMDARs to ERK activation [24], and NMDA-induced ERK signaling is mediated by NR2B subunit [25]. In this study, **5q** was evaluated for the effects on the NR2B and the p-ERK1/2 expression. The results showed that NMDA could increase the NR2B expression and down-regulate the p-ERK1/2 expression, but pretreatment with **5q** could suppress the NR2B up-regulation and increase p-ERK1/2 expression. Therefore, the NMDAR-ERK signaling cascade and NR2B-NMDARs were likely to be involved in the protective effect of **5q**.

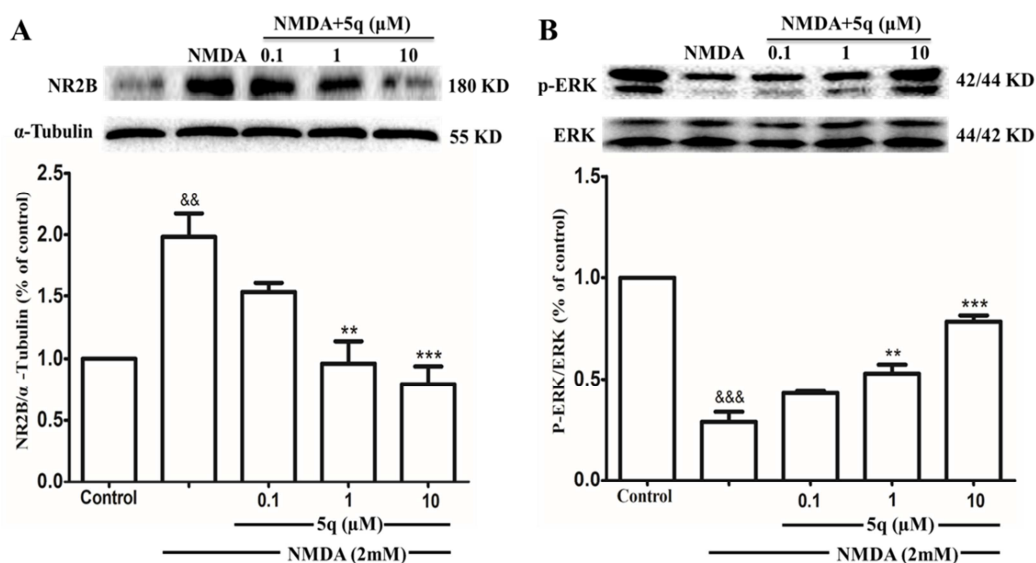


Figure 3. Western-blot analysis of NR2B and p-ERK1/2. (A) The expression of NR2B. (B) The expression of p-ERK/ERK. Data were presented as means \pm S.E.M. ($n = 3$). && $p < 0.01$ and &&& $p < 0.001$ compared with control group. ** $p < 0.01$ and *** $p < 0.001$ compared with NMDA-treated group.

2.5. Binding affinity study through docking with NR2B subunit of NMDARs

To rationalize the obtained biological results, computational molecular docking methods were used to predict the potential molecular interaction mechanisms between **5q** and NR2B-NMDARs. **5q** was docked at the NR1-NR2B subunit interface, the docking poses of **5q** were examined and the pose which had the highest Libdockscore was shown in **Figure 4**. The docking results showed that **5q** could fit well in the active pocket of NR2B-selective NMDAR antagonists but the orientation and interactions network of **5q** (yellow) were different from **1** (green), especially the hydrophobic aromatic part **A**, but it was very surprising that this part could almost overlap with **4** (purple). The parts **B** of **5q** and **1** had the similar interactions with NR1-NR2B subunit interface. These results indicated that **5q** might occupy the binding pocket of **4** and interacted with some residues in the binding pocket of **1** simultaneously. The docking result was consistent with the biological results. When the length of the alkyl spacer between the acylamino and the benzene ring of the part **B** was 2 methylene moieties, the part **B** of **5q** would occupy the pocket of **1** and place its phenyl ring in parallel to the part **B** of **1**, and the hydroxyl group (OH) was able to

form the hydrogen bonding interaction with the residues of NR2B (TYR 175, PHE 176 and GLU 236). The docking results suggested that **5q** might interact with NR2B-NMDARs in outstanding ways.

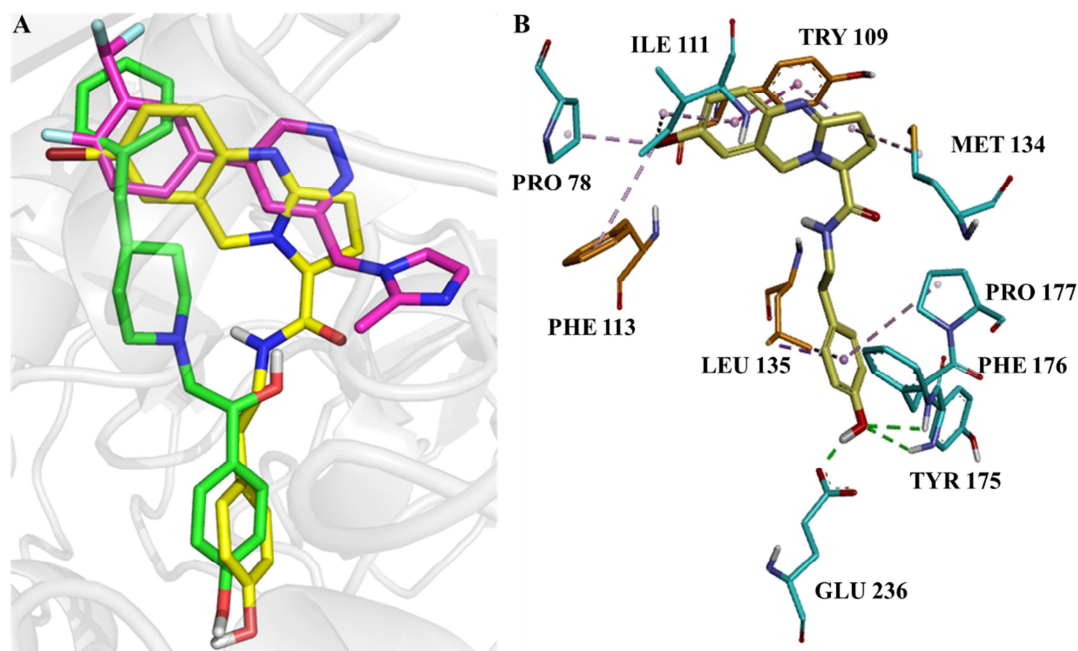


Figure 4. Docking poses of compound **5q** at the NMDA receptor (PDB code 5EWJ). (A) **1** (Ifenprodil, green), **4** (EVT-101, purple), **5q** (yellow). (B) The residues that interact with **5q**, the residues are colored in orange (NR1) and cyan (NR2B).

2.6. In Vitro Metabolic Stability Study

Based on the results of the in vitro neuroprotective activity, the compound **5q** was selected for the in vitro metabolic stability study and **1** was selected as the control medicine. As shown in **Table 3**, **1** showed weak stability with a clearance rate of 108.6 $\mu\text{L}/\text{min}/\text{mg}$ in human liver microsomes, while the compound **5q** exhibited higher metabolic stability with a clearance rate of 46.3 $\mu\text{L}/\text{min}/\text{mg}$, the ester derivative **16b** exhibited much lower metabolic stability with a clearance rate of 1183.2 $\mu\text{L}/\text{min}/\text{mg}$.

Table 3. In vitro metabolic stability study of **5q**, **16b** and **1**

Compd.	Human Liver Microsomes		
	$T_{1/2}$ (min)	CL ($\mu\text{L}/\text{min}/\text{mg}$)	Remaining (*NCF=60 min)
5q	29.9	46.3	99.3%
16b	1.2	1183.2	3.2%
1	12.8	108.6	87.3%

*NCF: the abbreviation of no co-factor. No NADPH regenerating system is added into NCF sample (replaced by buffer) during the 60 min-incubation.

3. Conclusions

Diverse 1,2,3,9-tetrahydropyrrolo[2,1-b]quinazoline-1-carboxylic acid derivatives were synthesized and their neuroprotective activity against NMDA-induced cytotoxicity in vitro varied from moderate to excellent. In addition, the Ca^{2+} influx induced by NMDA could be attenuated significantly when the SH-SY5Y cells were pretreated with **5q**, and **5q** could suppress the NR2B up-regulation and increase p-ERK1/2 expression. Moreover, the docking results showed that **5q** might fit well in the binding pocket of **4** and has specific key interactions with some residues in the binding pocket of **1** simultaneously and the results were consistent with the biological results. According to the experiments results in this study, it is feasible to conclude that NR2B-NMDARs might be involved in the protective effect of **5q** against to NMDA-induced neuron impairments. Besides, the compound **5q** exhibited acceptable metabolic stability. Although further studies are needed to reveal the mechanistic details, the extraordinary structure, the distinct interaction mode with NR2B-NMDARs and the metabolic stability of **5q** made it a promising lead for the development of new potent and orally bioavailable NR2B-selective NMDAR antagonists.

4. Experimental section

4.1. Chemistry

All commercially available reagents and solvents were used without further purification. TLC was performed on silica gel plates (Indicator F-254) and visualized by UV-light. NMR spectra were recorded on Bruker 400 MHz and 600 MHz instruments, and the chemical shifts were reported in terms of parts per million with TMS as the internal reference and coupling constants were reported in Hertz. High-resolution accurate mass determinations (HRMS) for all final target compounds were obtained on a Bruker Micromass Time of Flight mass spectrometer equipped with electrospray ionisation (ESI). Column chromatography was performed with silica gel (200-300 mesh).

4.1.1 General procedure for the preparation of compounds **10a–10d**

An ethanol solution (400 mL) of 2-nitrobenzaldehyde **7a** or 5-bromo-2-nitrobenzaldehyde **7b** (300 mmol) was dropwise to an aqueous solution of L-glutamic acid (or D-glutamic acid, 315 mmol) and sodium hydroxide (2 M, 300 mL) at room temperature. The mixture was stirred at room temperature for 1 h and cooled to 0~5 °C. Sodium borohydride (450 mmol) was added in small portions at 0~5 °C, and the mixture was then warmed up to room temperature and stirred for 3 h. The resulting solution was evaporated under vacuum till its volume was reduced to 300 mL, and then extracted with diethyl ether (70 mL × 3). The aqueous layer was acidified to pH 4~5 with concentrated hydrochloric acid. The resulting suspension of **8a–8b** (or **8c–8d**) was filtered and then heated in refluxing ethanol (800 mL) for 5 h. This solution was then filtered and concentrated in vacuum to give an ivory-white dusty solid **9a–9b** (or **9c–9d**), which were used in the next reaction without further purification. To the ethanol solution (600 mL) of the above crude intermediates **9a–9b** (or **9c–9d**), activated carbon (6.0 g) and ferric chloride hexahydrate (0.05 g) were added. The suspension was then heated to 50 °C and hydrazine hydrate (1200 mmol) was added dropwise. This mixture was heated at reflux for approximately 72 h. At this point, the mixture was filtered and the solvent was removed by vacuum evaporation. The residue was purified by flash chromatography on silica gel using methanol–ethyl acetate (5:4 v/v) to give compounds **10a–10b** (or **10c–10d**).

4.1.2. (*S*)-*N*-benzyl-1,2,3,9-tetrahydropyrrolo[2,1-*b*]quinazoline-1-carboxamide (**5a**)

To a solution of **10a** (1.0g, 4.6 mmol) and triethylamine (1.3mL, 9.3 mmol) in anhydrous DMF (10 mL) was added Bis(2-oxo-3-oxazolidinyl)phosphonic chloride (BOP-Cl) (1.4g, 5.5 mmol) at 0 °C, the mixture was stirred for 0.5 h at this temperature, then phenylmethanamine (0.6mL, 5.5mmol) was added, stirred for 5h at room temperature. Added 30mL H₂O and stirred for 1 h, the solution was filtered and gave a white solid 0.6g, yield: 42.7%. ¹H-NMR (DMSO-*d*₆, 600 MHz) δ: 8.81~8.79 (t, J=6.0 Hz, 1H), 7.36~7.33 (t, J=7.8Hz, 2H), 7.28~7.24 (m, 3H), 7.10~7.07 (m, 1H), 6.92~6.91 (m, 2H), 6.84~6.83 (d, J=7.8 Hz, 1H), 4.46~4.43 (d, J=13.2 Hz, 1H), 4.41~4.38 (d, J=13.2 Hz, 1H), 4.34~4.33 (m, 2H), 4.05~4.03 (m, 1H), 2.60~2.55 (m,

1H), 2.51~2.46 (m, 1H), 2.28~2.23 (m, 1H), 1.89~1.84 (m, 1H). ¹³C-NMR (DMSO-*d*₆, 150 MHz) δ: 170.09, 162.43, 139.02, 128.27 (3C), 127.81, 127.13 (3C), 126.80, 125.98, 123.39, 119.58, 64.01, 44.80, 42.06, 29.46, 23.89. ESI-HRMS: calcd for C₁₉H₂₀N₃O, [M + H]⁺, 306.1606, found 306.1598.

4.1.3.

(S)-*N*-(4-hydroxybenzyl)-1,2,3,9-tetrahydropyrrolo[2,1-*b*]quinazoline-1-carboxamide (**5b**)

Yield: 43.5%; ¹H-NMR (DMSO-*d*₆, 400 MHz) δ: 9.19 (s, 1H), 8.25 (s, 1H), 7.07 (br, 1H), 7.00~6.99 (d, J=8.4 Hz, 2H), 6.93~6.90 (m, 2H), 6.82~6.80 (d, J=8.0 Hz, 1H), 6.69~6.67 (d, J=8.4 Hz, 2H), 4.32~4.29 (d, J=13.2 Hz, 1H), 4.22~4.19 (d, J=13.6 Hz, 1H), 3.90~3.86 (m, 1H), 2.65~2.62 (m, 2H), 2.55~2.39 (m, 2H), 2.20~2.11 (m, 1H), 1.78~1.76 (m, 1H). ¹³C-NMR (DMSO-*d*₆, 150 MHz) δ: 170.37, 162.97, 156.14, 143.74, 130.07 (2C), 129.70, 128.33, 126.55, 123.86, 123.81, 120.25, 115.50 (2C), 64.60, 45.27, 34.59, 30.04, 24.31. ESI-HRMS: calcd for C₁₉H₂₀N₃O₂, [M + H]⁺, 322.1556; found 322.1549.

4.1.4.

(S)-*N*-(4-methoxybenzyl)-1,2,3,9-tetrahydropyrrolo[2,1-*b*]quinazoline-1-carboxamide (**5c**)

Yield: 45.1%; ¹H-NMR (DMSO-*d*₆, 600 MHz) δ: 8.72~8.71 (m, 1H), 7.21~7.19 (d, J=8.4 Hz, 2H), 7.09~7.07 (m, 1H), 6.92~6.89 (m, 4H), 6.83~6.82 (d, J=7.8 Hz, 1H), 4.44~4.41 (d, J=13.2 Hz, 1H), 4.39~4.37 (d, J=13.2 Hz, 1H), 4.26~4.25 (m, 2H), 4.01~3.99 (m, 1H), 3.73 (s, 3H), 2.59~2.53 (m, 1H), 2.50~2.45 (m, 1H), 2.25~2.21 (m, 1H), 1.86~1.82 (m, 1H). ¹³C-NMR (DMSO-*d*₆, 150 MHz) δ: 169.98, 162.40, 158.17, 143.19, 130.96 (2C), 128.51, 127.78, 125.97, 123.30, 123.28, 119.65, 113.66 (2C), 63.94, 54.95, 44.79, 41.53, 29.48, 23.86. ESI-HRMS: calcd for C₂₀H₂₂N₃O₂, [M + H]⁺, 336.1712, found 336.1703.

4.1.5.

(S)-*N*-(4-fluorobenzyl)-1,2,3,9-tetrahydropyrrolo[2,1-*b*]quinazoline-1-carboxamide (**5d**)

Yield: 43.1%; ¹H-NMR (DMSO-*d*₆, 600 MHz) δ: 8.81~8.80 (t, J=6.0 Hz, 1H),

7.33~7.30 (m, 2H), 7.18~7.16 (t, J=8.4 Hz, 2H), 7.10~7.07 (m, 1H), 6.92~6.91 (m, 2H), 6.84~6.82 (d, J=7.8 Hz, 1H), 4.44~4.42 (d, J=13.2 Hz, 1H), 4.39~4.37 (d, J=13.2 Hz, 1H), 4.31~4.30 (d, J=6.0 Hz, 2H), 4.02~4.00 (m, 1H), 2.58~2.45 (m, 2H), 2.26~2.21 (m, 1H), 1.87~1.82(m, 1H). ^{13}C -NMR (DMSO- d_6 , 150 MHz) δ : 170.78, 162.97, 161.69 (d, J=242 Hz), 143.81, 135.87, 129.76, 129.71, 128.37, 126.55, 123.90 (2C), 120.26, 115.66, 115.52, 64.53, 45.40, 41.95, 30.05, 24.47. ESI-HRMS: calcd for $\text{C}_{19}\text{H}_{20}\text{FN}_3\text{O}$, $[\text{M} + \text{H}]^+$, 324.1512, found 324.1506.

4.1.6.

(S)-*N*-(4-methylbenzyl)-1,2,3,9-tetrahydropyrrolo[2,1-*b*]quinazoline-1-carboxamide (**5e**)

Yield: 45.4%; ^1H -NMR (DMSO- d_6 , 600 MHz) δ : 8.75~8.73 (t, J=6.0 Hz, 1H), 7.17~7.14 (m, 4H), 7.09~7.07 (m, 1H), 6.92~6.91 (m, 2H), 6.83~6.82 (d, J=7.8 Hz, 1H), 4.44~4.42 (d, J=13.2 Hz, 1H), 4.39~4.37 (d, J=13.2 Hz, 1H), 4.28~4.27 (m, 2H), 4.02~4.00 (m, 1H), 2.58~2.45 (m, 2H), 2.28 (s, 3H), 2.26~2.20 (m, 1H), 1.88~1.82 (m, 1H). ^{13}C -NMR (DMSO- d_6 , 150 MHz) δ : 170.65, 162.98, 143.81, 136.60, 136.45, 129.40 (3C), 128.37, 127.73 (2C), 126.55, 123.89, 120.25, 64.53, 45.39, 42.40, 30.06, 24.46, 21.15. ESI-HRMS: calcd for $\text{C}_{20}\text{H}_{22}\text{N}_3\text{O}$, $[\text{M} + \text{H}]^+$, 320.1763, found 320.1748.

4.1.7.

(S)-7-bromo-*N*-(4-hydroxybenzyl)-1,2,3,9-tetrahydropyrrolo[2,1-*b*]quinazoline-1-carboxamide (**5f**)

Yield: 48.1%; ^1H -NMR (DMSO- d_6 , 600 MHz) δ : 9.34 (s, 1H), 8.67 (s, 1H), 7.24~7.23 (m, 1H), 7.16 (s, 1H), 7.08~7.07 (m, 2H), 6.76~6.71 (m, 3H), 4.44~4.42 (d, J=13.8 Hz, 1H), 4.39~4.36 (d, J=13.8 Hz, 1H), 4.20~4.20 (m, 2H), 4.01 (s, 1H), 2.56~2.46 (m, 2H), 2.24~2.21 (m, 1H), 1.84 (s, 1H). ^{13}C -NMR (DMSO- d_6 , 150 MHz) δ : 170.32, 163.72, 156.84, 143.36, 131.10, 129.63, 129.17, 129.14 (2C), 125.71, 122.87, 115.58 (2C), 115.16, 64.46, 44.87, 42.27, 30.14, 24.46. ESI-HRMS: calcd for $\text{C}_{19}\text{H}_{19}\text{BrN}_3\text{O}_2$, $[\text{M} + \text{H}]^+$, 400.0661, 402.0640; found 400.0670, 402.0650.

4.1.8.

(S)-7-bromo-*N*-(4-methoxybenzyl)-1,2,3,9-tetrahydropyrrolo[2,1-*b*]quinazoline-1-carboxamide (**5g**)

Yield: 40.1%; $^1\text{H-NMR}$ ($\text{DMSO-}d_6$, 600 MHz) δ : 8.73 (s, 1H), 7.24~7.16 (m, 4H), 6.91~6.90 (m, 2H), 6.76~6.75 (m, 1H), 4.44~4.36 (m, 2H), 4.26 (s, 2H), 4.01 (s, 1H), 3.73 (s, 3H), 2.55~2.50 (m, 2H), 2.23 (s, 1H), 1.84 (s, 1H). $^{13}\text{C-NMR}$ ($\text{DMSO-}d_6$, 150 MHz) δ : 170.39, 163.71, 158.77, 143.29, 131.47, 131.12, 129.18, 129.11 (2C), 125.69, 122.85, 115.19, 114.26 (2C), 64.50, 55.54, 44.88, 42.14, 30.14, 24.47. ESI-HRMS: calcd for $\text{C}_{20}\text{H}_{21}\text{BrN}_3\text{O}_2$, $[\text{M} + \text{H}]^+$, 414.0817, 416.0797; found 414.0823, 416.0806.

4.1.9.

(S)-7-bromo-*N*-(4-fluorobenzyl)-1,2,3,9-tetrahydropyrrolo[2,1-*b*]quinazoline-1-carboxamide (**5h**)

Yield: 38.3%; $^1\text{H-NMR}$ ($\text{DMSO-}d_6$, 600 MHz) δ : 8.82~8.80 (t, $J=6.0$ Hz, 1H), 7.32~7.30 (m, 2H), 7.25~7.23 (m, 1H), 7.19~7.16 (m, 3H), 6.77~6.76 (d, $J=8.4$ Hz, 1H), 4.45~4.43 (d, $J=13.8$ Hz, 1H), 4.39~4.37 (d, $J=14.4$ Hz, 1H), 4.31~4.30 (d, $J=6.0$ Hz, 2H), 4.04~4.02 (m, 1H), 2.59~2.45 (m, 2H), 2.27~2.25 (m, 1H), 1.87~1.82 (m, 1H). $^{13}\text{C-NMR}$ ($\text{DMSO-}d_6$, 150 MHz) δ : 170.59, 163.71, 161.70 (d, $J=243$ Hz), 143.21, 135.79, 131.13, 129.77, 129.72, 129.19, 125.68, 122.85, 115.68, 115.54, 115.23, 64.51, 44.91, 41.97, 30.12, 24.49. ESI-HRMS: calcd for $\text{C}_{19}\text{H}_{18}\text{BrFN}_3\text{O}$, $[\text{M} + \text{H}]^+$, 402.0617, 404.0597; found 402.0620, 404.0402.

4.1.10. *(S)*-*N*-phenyl-1,2,3,9-tetrahydropyrrolo[2,1-*b*]quinazoline-1-carboxamide (**5i**)

Yield: 43.4%; $^1\text{H-NMR}$ ($\text{DMSO-}d_6$, 600MHz) δ : 10.33 (s, 1H), 7.65~7.64 (m, 2H), 7.34~7.32 (t, $J=7.8$ Hz, 2H), 7.12~7.07 (m, 2H), 6.95~6.91 (m, 2H), 6.87~6.85 (d, $J=7.8$ Hz, 1H), 4.53~4.50 (d, $J=13.2$ Hz, 1H), 4.48~4.46 (d, $J=13.2$ Hz, 1H), 4.23~4.21 (m, 1H), 2.65~2.60 (m, 1H), 2.57~2.52 (m, 1H), 2.36~2.30 (m, 1H), 2.00~1.95 (m, 1H). $^{13}\text{C-NMR}$ ($\text{DMSO-}d_6$, 150 MHz) δ : 169.52, 163.07, 143.25, 139.09, 129.27 (2C), 128.44, 126.64, 124.22, 124.08, 123.65, 120.13, 119.92 (2C), 65.09, 45.38, 30.01, 24.60. ESI-HRMS: calcd for $\text{C}_{18}\text{H}_{18}\text{N}_3\text{O}$, $[\text{M} + \text{H}]^+$, 292.1450; found 292.1456.

4.1.11.

(S)-*N*-(4-hydroxyphenyl)-1,2,3,9-tetrahydropyrrolo[2,1-*b*]quinazoline-1-carboxamide

(5j)

Yield: 45.1%; ¹H-NMR (DMSO-*d*₆, 400 MHz) δ: 10.05 (s, 1H), 9.26 (s, 1H), 7.43~7.41 (d, J=8.8 Hz, 2H), 7.12~7.07 (m, 1H), 6.95~6.91 (m, 2H), 6.86~6.84 (d, J=7.6 Hz, 1H), 6.73~6.71 (d, J=8.8 Hz, 2H), 4.51~4.43 (m, 2H), 4.15~4.12 (m, 1H), 2.65~2.48 (m, 2H), 2.32~2.27 (m, 1H), 1.99~1.91 (m, 1H). ¹³C-NMR (DMSO-*d*₆, 150 MHz) δ: 168.80, 163.01, 154.14, 143.75, 130.70, 128.38, 126.59, 123.91, 123.86, 121.66 (2C), 120.23, 115.56 (2C), 64.95, 45.35, 30.08, 24.54. ESI-HRMS: calcd for C₁₈H₁₈N₃O₂, [M + H]⁺, 308.1399; found 308.1390.

4.1.12.

(S)-*N*-(4-methoxyphenyl)-1,2,3,9-tetrahydropyrrolo[2,1-*b*]quinazoline-1-carboxamide

(5k)

Yield: 51.2%; ¹H-NMR (DMSO-*d*₆, 600 MHz) δ: 10.20 (s, 1H), 7.56~7.54 (m, 2H), 7.12~7.09 (m, 1H), 6.96~6.89 (m, 4H), 6.87~6.85 (d, J=7.2 Hz, 1H), 4.53~4.50 (d, J=13.2 Hz, 2H), 4.48~4.45 (d, J=13.8 Hz, 1H), 4.22~4.18 (m, 1H), 3.72 (s, 3H), 2.66~2.53 (m, 2H), 2.33~2.31 (m, 1H), 2.00~1.94 (m, 1H). ¹³C-NMR (DMSO-*d*₆, 150 MHz) δ: 168.89, 163.12, 156.00, 132.17, 128.47, 126.67, 124.14, 123.46, 121.47 (2C), 120.06, 114.36 (3C), 65.11, 55.65, 45.37, 30.03, 24.56. ESI-HRMS: calcd for C₁₈H₁₈N₃O, [M + H]⁺, 322.1556; found 322.1566.

4.1.13.

(S)-7-bromo-*N*-(4-hydroxyphenyl)-1,2,3,9-tetrahydropyrrolo[2,1-*b*]quinazoline-1-carboxamide (5l)

Yield: 35.7%; ¹H-NMR (DMSO-*d*₆, 400 MHz) δ: 10.04 (s, 1H), 9.24 (s, 1H), 7.41~7.49 (d, J=8.4 Hz, 2H), 7.24~7.22 (d, J=8.4 Hz, 1H), 7.16 (s, 1H), 6.77~6.69 (m, 3H), 4.49~4.40k (m, 2H), 4.12 (s, 1H), 2.60~2.49 (m, 2H), 2.30~2.25 (m, 1H), 1.94 (s, 1H). ¹³C-NMR (DMSO-*d*₆, 150 MHz) δ: 167.98, 163.12, 153.54, 142.64, 130.51, 130.03, 128.59, 125.07, 122.23, 121.06 (2C), 114.95 (2C), 114.59, 64.31, 44.24, 29.53, 23.91. ESI-HRMS: calcd for C₁₈H₁₇BrN₃O₂, [M + H]⁺, 386.0504, 388.0484; found 386.0495, 388.0476.

4.1.14. *(S)*-*N*-phenethyl-1,2,3,9-tetrahydropyrrolo[2,1-*b*]quinazoline-1-carboxamide (5m)

Yield: 44.1%; $^1\text{H-NMR}$ (DMSO- d_6 , 600 MHz) δ : 8.32~8.30 (t, $J=6.0$ Hz, 1H), 7.31~7.29 (t, $J=7.8$ Hz, 2H), 7.23~7.20 (m, 3H), 7.09~7.06 (t, $J=7.2$ Hz, 1H), 6.93~6.88 (m, 2H), 6.82~6.81 (d, $J=7.8$ Hz, 1H), 4.32~4.30 (d, $J=13.2$ Hz, 1H), 4.22~4.19 (d, $J=13.8$ Hz, 1H), 3.90~3.87 (m, 1H), 3.39~3.35 (m, 2H), 2.80~2.72 (m, 2H), 2.54~2.48 (m, 1H), 2.46~2.41 (m, 1H), 2.18~2.12 (m, 1H), 1.77~1.71 (m, 1H). $^{13}\text{C-NMR}$ (DMSO- d_6 , 150 MHz) δ : 169.83, 162.35, 143.07, 139.12, 128.61 (2C), 128.13 (2C), 127.72, 125.97, 125.90, 123.26, 123.19, 119.61, 63.98, 44.64, 34.77, 29.41, 23.71. ESI-HRMS: calcd for $\text{C}_{20}\text{H}_{22}\text{N}_3\text{O}$, $[\text{M} + \text{H}]^+$, 320.1763, found 320.1755.

4.1.15.

(S)-N-(4-hydroxyphenethyl)-1,2,3,9-tetrahydropyrrolo[2,1-b]quinazoline-1-carboxamide (5n)

Yield: 38.1%; $^1\text{H-NMR}$ (DMSO- d_6 , 400 MHz) δ : 9.19 (s, 1H), 8.25 (s, 1H), 7.09~7.05 (m, 1H), 7.01~6.99 (d, $J=8.0$ Hz, 2H), 6.93~6.90 (m, 2H), 6.82~6.80 (d, $J=8.0$ Hz, 1H), 6.69~6.67 (d, $J=8.0$ Hz, 2H), 4.32~4.29 (d, $J=13.6$ Hz, 1H), 4.22~4.18 (d, $J=13.6$ k Hz, 1H), 3.89~3.86 (m, 1H), 3.33~3.28 (m, 2H), 2.65~2.62 (m, 2H), 2.50~2.39 (m, 2H), 2.20~2.11 (m, 1H), 1.80~1.71 (m, 1H). $^{13}\text{C-NMR}$ (DMSO- d_6 , 150 MHz) δ : 170.32, 162.89, 156.06, 143.73, 130.00 (2C), 129.63, 128.25, 126.47, 123.78 (2C), 120.19, 115.43 (2C), 64.52, 45.20, 40.67, 34.52, 29.98, 24.24. ESI-HRMS: calcd for $\text{C}_{20}\text{H}_{22}\text{N}_3\text{O}_2$, $[\text{M} + \text{H}]^+$, 336.1712, found 336.1705.

4.1.16.

(S)-N-(4-methoxyphenethyl)-1,2,3,9-tetrahydropyrrolo[2,1-b]quinazoline-1-carboxamide (5o)

Yield: 46.2%; $^1\text{H-NMR}$ (DMSO- d_6 , 600 MHz) δ : 8.28~8.26 (m, 1H), 7.14~7.12 (d, $J=8.4$ Hz, 2H), 7.08~7.06 (t, $J=6.6$ Hz, 1H), 6.92~6.90 (t, $J=7.2$ Hz, 1H), 6.88~6.85 (m, 3H), 6.82~6.81 (d, $J=7.2$ Hz, 1H), 4.31~4.29 (d, $J=13.2$ Hz, 1H), 4.19~4.17 (d, $J=13.8$ Hz, 1H), 3.89~3.87 (m, 1H), 3.71 (s, 3H), 3.37~3.27 (m, 2H), 2.73~2.65 (m, 2H), 2.54~2.49 (m, 1H), 2.46~2.41 (m, 1H), 2.18~2.12 (m, 1H), 1.78~1.73 (m, 1H). $^{13}\text{C-NMR}$ (DMSO- d_6 , 150 MHz) δ : 169.34, 161.88, 157.07, 142.72, 130.47, 129.10 (2C), 127.25, 125.40, 122.77, 122.74, 119.17, 113.07 (2C), 63.51, 54.35, 44.17, 39.54, 33.44, 28.96, 23.21. ESI-HRMS: calcd for $\text{C}_{21}\text{H}_{24}\text{N}_3\text{O}$, $[\text{M} + \text{H}]^+$, 350.1869; found

350.1874.

4.1.17

(S)-N-(4-fluorophenethyl)-1,2,3,9-tetrahydropyrrolo[2,1-b]quinazoline-1-carboxamide (5p)

Yield: 40.1%; ¹H-NMR (DMSO-*d*₆, 600 MHz) δ: 8.29~8.28 (t, J=5.4 Hz, 1H), 7.26~7.24 (m, 2H), 7.13~7.10 (t, J=9.0 Hz, 2H), 7.09~7.06 (t, J=7.2 Hz, 1H), 6.92~6.90 (t, J=7.2 Hz, 1H), 6.88~6.87 (d, J=7.2 Hz, 1H), 6.82~6.81 (d, J=7.8 Hz, 1H), 4.31~4.29 (d, J=13.2 Hz, 1H), 4.18~4.16 (d, J=13.2 Hz, 1H), 3.88~3.86 (m, 1H), 3.40~3.34 (m, 2H), 2.79~2.71 (m, 2H), 2.52~2.48 (m, 1H), 2.46~2.39 (m, 1H), 2.18~2.12 (m, 1H), 1.76~1.70 (m, 1H). ¹³C-NMR (DMSO-*d*₆, 150 MHz) δ: 170.49, 162.95, 161.33 (d, J=240 Hz), 143.79, 135.89, 131.05, 131.00, 128.34, 126.46, 123.88, 123.86, 120.23, 115.47, 115.33, 64.58, 45.25, 34.49, 30.03, 24.33. ESI-HRMS: calcd for C₂₀H₂₁FN₃O, [M + H]⁺, 338.1669; found 338.1676.

4.1.18.

(S)-7-bromo-N-(4-hydroxyphenethyl)-1,2,3,9-tetrahydropyrrolo[2,1-b]quinazoline-1-carboxamide (5q)

Yield: 43.8%; ¹H-NMR (DMSO-*d*₆, 600 MHz) δ: 9.19 (s, 1H), 8.28~8.26 (t, J=6.0 Hz, 1H), 7.24~7.22 (m, 1H), 7.13~7.13 (m, 1H), 7.00~6.99 (d, J=8.4 Hz, 2H), 6.75~6.74 (d, J=8.4 Hz, 1H), 6.69~6.67 (d, J=7.8 Hz, 2H), 4.33~4.31 (d, J=14.4 Hz, 1H), 4.23~4.20 (d, J=14.4 Hz, 1H), 3.90~3.88 (m, 1H), 3.31~3.26 (m, 2H), 2.64~2.61 (t, J=7.2 Hz, 2H), 2.47~2.39 (m, 2H), 2.19~2.13 (m, 1H), 1.77~1.72 (m, 1H). ¹³C-NMR (DMSO-*d*₆, 150 MHz) δ: 170.21, 163.68, 156.15, 143.36, 131.08, 130.07 (2C), 129.69, 129.14, 125.70, 122.87, 115.51 (2C), 115.15, 64.53, 46.16, 44.79, 34.62, 30.12, 24.34. ESI-HRMS: calcd for C₂₀H₂₁BrN₃O₂, [M + H]⁺, 414.0817, 416.0797; found 414.0814, 416.0797.

4.1.19.

(S)-N-(3-phenylpropyl)-1,2,3,9-tetrahydropyrrolo[2,1-b]quinazoline-1-carboxamide (5r)

Yield: 42.9%; ¹H-NMR (DMSO-*d*₆, 600 MHz) δ: 8.32~8.30 (m, 1H), 7.30~7.27 (d, J=7.8 Hz, 2H), 7.22~7.17 (m, 3H), 7.09~7.07 (m, 1H), 6.93~6.89 (m, 2H), 6.83~6.82

(d, $J=7.2$ Hz, 1H), 4.43~4.41 (d, $J=13.2$ Hz, 1H), 4.38~4.36 (d, $J=13.8$ Hz, 1H), 3.96~3.94 (m, 1H), 3.14~3.12 (m, 2H), 2.60~2.45 (m, 4H), 2.24~2.19 (m, 1H), 1.85~1.80 (m, 1H), 1.76~1.71 (m, 2H). ^{13}C -NMR (DMSO- d_6 , 150 MHz) δ : 170.54, 163.01, 143.85, 142.09, 128.78 (4C), 128.35, 126.54, 126.25, 123.88, 123.86, 120.25, 64.58, 45.34, 38.70, 32.97, 31.31, 30.08, 24.46. ESI-HRMS: calcd for $\text{C}_{21}\text{H}_{24}\text{N}_3\text{O}$, $[\text{M} + \text{H}]^+$, 334.1919; found 334.1930.

4.1.20.

(S)-7-bromo-*N*-(3-phenylpropyl)-1,2,3,9-tetrahydropyrrolo[2,1-*b*]quinazoline-1-carboxamide (**5s**)

Yield: 55.3%; ^1H -NMR (DMSO- d_6 , 600 MHz) δ : 8.32 (s, 1H), 7.30~7.27 (m, 2H), 7.24~7.16 (m, 5H), 6.76~6.75 (d, $J=8.4$ Hz, 1H), 4.43~4.41 (d, $J=13.8$ Hz, 1H), 4.38~4.35 (d, $J=13.8$ Hz, 1H), 3.97~3.95 (m, 1H), 3.14~3.10 (m, 2H), 2.60~2.44 (m, 4H), 2.25~2.19 (m, 1H), 1.84~1.80 (m, 1H), 1.75~1.72 (m, 2H). ^{13}C -NMR (DMSO- d_6 , 150 MHz) δ : 170.36, 163.73, 143.39, 142.08, 131.09, 129.17, 128.79 (2C), 128.77 (2C), 126.25, 125.72, 122.88, 115.14, 64.55, 44.85, 38.71, 32.97, 31.28, 30.16, 24.47. ESI-HRMS: calcd for $\text{C}_{21}\text{H}_{23}\text{BrN}_3\text{O}$, $[\text{M} + \text{H}]^+$, 412.1024, 414.1004; found 412.1013, 414.1013.

4.1.21.

(R)-*N*-(4-hydroxybenzyl)-1,2,3,9-tetrahydropyrrolo[2,1-*b*]quinazoline-1-carboxamide (**12a**)

Yield: 39.9%; ^1H -NMR (DMSO- d_6 , 400 MHz) δ : 9.31 (s, 1H), 8.65 (s, 1H), 7.08~7.06 (m, 3H), 6.92~6.91 (m, 2H), 6.83~6.81 (d, $J=7.6$ Hz, 1H), 6.73~6.71 (d, $J=8.0$ Hz, 2H), 4.44~4.35 (m, 2H), 4.21~4.20 (m, 2H), 4.01~3.98 (m, 1H), 2.61~2.43 (m, 2H), 2.26~2.19 (m, 1H), 1.88~1.80 (m, 1H). ^{13}C -NMR (DMSO- d_6 , 150 MHz) δ : 169.89, 162.40, 156.23, 143.19, 129.12, 128.54 (2C), 127.77, 125.95, 123.28, 123.25, 119.64, 114.96 (2C), 63.91, 44.76, 41.65, 29.47, 23.83. ESI-HRMS: calcd for $\text{C}_{19}\text{H}_{20}\text{N}_3\text{O}_2$, $[\text{M} + \text{H}]^+$, 322.1556; found 322.1549.

4.1.22.

(R)-*N*-(4-methoxybenzyl)-1,2,3,9-tetrahydropyrrolo[2,1-*b*]quinazoline-1-carboxamide (**12b**)

Yield: 46.1%; ¹H-NMR (DMSO-*d*₆, 600 MHz) δ: 8.72~8.71 (t, J=6.0 Hz, 1H), 7.21~7.19 (d, J=9.0 Hz, 2H), 7.09~7.07 (m, 1H), 6.92~6.89 (m, 4H), 6.83~6.82 (d, J=7.8 Hz, 1H), 4.44~4.41 (d, J=13.2 Hz, 1H), 4.39~4.37 (d, J=13.2 Hz, 1H), 4.26~4.25 (m, 2H), 4.01~3.99 (m, 1H), 3.73 (s, 3H), 2.57~2.53 (m, 1H), 2.50~2.47 (m, 1H), 2.26~2.21 (m, 1H), 1.87~1.81 (m, 1H). ¹³C-NMR (DMSO-*d*₆, 150 MHz) δ: 170.54, 163.01, 158.76, 143.62, 131.54, 129.10 (2C), 128.39, 126.57, 123.93, 123.78, 120.20, 114.25 (2C), 64.55, 55.53, 45.37, 42.12, 30.06, 24.45. ESI-HRMS: calcd for C₂₀H₂₁N₃O₂, [M + H]⁺, 336.1712; found 336.1712.

4.1.23.

(R)-*N*-(4-fluorobenzyl)-1,2,3,9-tetrahydropyrrolo[2,1-*b*]quinazoline-1-carboxamide (**12c**)

Yield: 45.9%; ¹H-NMR (DMSO-*d*₆, 600 MHz) δ: 8.81~8.79 (t, J=6.0 Hz, 1H), 7.33~7.30 (m, 2H), 7.19~7.15 (m, 2H), 7.10~7.07(m, 1H), 6.92~6.90 (m, 2H), 6.84~6.82 (d, J=7.8 Hz, 1H), 4.45~4.42 (d, J=13.2 Hz, 1H), 4.39~4.37 (d, J=13.8 Hz, 1H), 4.31~4.30 (m, 2H), 4.03~4.00 (m, 1H), 2.61~2.54 (m, 1H), 2.51~2.45 (m, 1H), 2.27~2.21 (m, 1H), 1.88~1.82 (m, 1H). ¹³C-NMR (DMSO-*d*₆, 150 MHz) δ: 170.76, 163.00, 161.70 (d, J=242 Hz), 143.67, 135.87, 129.77, 129.71, 128.38, 126.56, 123.94, 123.83, 120.23, 115.66, 115.52, 64.56, 45.40, 41.96, 30.04, 24.47. ESI-HRMS: calcd for C₁₉H₁₉FN₃O, [M + H]⁺, 324.1512; found 324.1514.

4.1.24.

(R)-7-bromo-*N*-(4-hydroxybenzyl)-1,2,3,9-tetrahydropyrrolo[2,1-*b*]quinazoline-1-carboxamide (**12d**)

Yield: 47.1%; ¹H-NMR (DMSO-*d*₆, 600 MHz) δ: 9.34 (s, 1H), 8.68 (s, 1H), 7.25~7.23 (m, 1H), 7.17 (s, 1H), 7.08~7.07 (m, 2H), 6.77~6.71 (m, 3H), 4.45~4.37 (m, 2H), 4.21~4.20 (m, 2H), 4.02 (s, 1H), 2.57~2.50 (m, 2H), 2.23 (s, 1H), 1.85 (s, 1H). ¹³C-NMR (DMSO-*d*₆, 150 MHz) δ: 170.24, 163.76, 156.85, 142.94, 131.15, 129.61, 129.22, 129.14 (2C), 125.50, 122.77, 115.58 (2C), 115.28, 64.54, 44.87, 42.28, 30.13, 24.47. ESI-HRMS: calcd for C₁₉H₁₉BrN₃O₂, [M + H]⁺, 400.0661, 402.0640; found 400.0666, 402.0649.

4.1.25.

(R)-N-(4-hydroxyphenyl)-1,2,3,9-tetrahydropyrrolo[2,1-b]quinazoline-1-carboxamide (12e)

Yield: 50.2%; ¹H-NMR (DMSO-*d*₆, 400 MHz) δ: 10.05 (s, 1H), 9.26 (s, 1H), 7.43~7.41 (d, J=8.8 Hz, 2H), 7.12~7.07 (m, 1H), 6.95~6.90 (m, 2H), 6.86~6.84 (d, J=7.6 Hz, 1H), 6.73~6.71 (d, J=8.8 Hz, 2H), 4.50~4.43 (m, 2H), 4.15~4.12 (m, 1H), 2.65~2.48 (m, 2H), 2.32~2.27 (m, 1H), 1.98~1.91 (m, 1H). ¹³C-NMR (DMSO-*d*₆, 150 MHz) δ: 168.21, 162.42, 153.54, 143.15, 130.10, 127.78, 126.00, 123.31, 123.26, 121.07 (2C), 119.64, 114.97 (2C), 64.35, 44.76, 29.48, 23.94. ESI-HRMS: calcd for C₁₈H₁₈N₃O₂, [M + H]⁺, 308.1399; found 308.1389.

4.1.26.

(R)-7-bromo-N-(4-hydroxyphenyl)-1,2,3,9-tetrahydropyrrolo[2,1-b]quinazoline-1-carboxamide (12f)

Yield: 35.6%; ¹H-NMR (DMSO-*d*₆, 400 MHz) δ: 10.05 (s, 1H), 9.25 (s, 1H), 7.42~7.40 (d, J=7.6 Hz, 2H), 7.25~7.17 (m, 2H), 6.78~6.70 (m, 3H), 4.51~4.41 (m, 2H), 4.14 (s, 1H), 2.67~2.50 (m, 2H), 2.32~2.27 (m, 1H), 1.95 (s, 1H). ¹³C-NMR (DMSO-*d*₆, 150 MHz) δ: 167.99, 163.15, 153.57, 142.63, 130.54, 130.06, 128.62, 125.08, 122.24, 121.08 (2C), 114.97 (2C), 114.63, 64.34, 44.27, 29.55, 23.93. ESI-HRMS: calcd for C₁₈H₁₇BrN₃O₂, [M + H]⁺, 386.0504, 388.0484; found 386.0496, 388.0478.

4.1.27.

(R)-N-(4-hydroxyphenethyl)-1,2,3,9-tetrahydropyrrolo[2,1-b]quinazoline-1-carboxamide (12g)

Yield: 40.1%; ¹H-NMR (DMSO-*d*₆, 400 MHz) δ: 9.19 (s, 1H), 8.25~8.23 (m, 1H), 7.09~7.05 (m, 1H), 7.01~6.99 (d, J=8.4 Hz, 2H), 6.93~6.88 (m, 2H), 6.82~6.80 (d, J=8.0 Hz, 1H), 6.69~6.67 (d, J=8.4 Hz, 2H), 4.32~4.29 (d, J=13.6 Hz, 1H), 4.22~4.19 (d, J=13.6 Hz, 1H), 3.90~3.87 (m, 1H), 3.32~3.23 (m, 2H), 2.65~2.62 (t, J=7.2 Hz, 2H), 2.56~2.40 (m, 2H), 2.20~2.11 (m, 1H), 1.80~1.72 (m, 1H). ¹³C-NMR (DMSO-*d*₆, 150 MHz) δ: 170.37, 162.97, 156.13, 143.73, 130.07 (2C), 129.70, 128.33, 126.55, 123.87, 123.81, 120.25, 115.50 (2C), 64.60, 45.27, 40.74, 34.59, 30.05, 24.31. ESI-HRMS: calcd for C₂₀H₂₂N₃O₂, [M + H]⁺, 336.1712; found 336.1707.

4.1.28.

(R)-7-bromo-*N*-(4-hydroxyphenethyl)-1,2,3,9-tetrahydropyrrolo[2,1-*b*]quinazoline-1-carboxamide (**12h**)

Yield: 40.5%; $^1\text{H-NMR}$ (DMSO- d_6 , 400 MHz) δ : 9.18 (s, 1H), 8.27~8.24 (t, $J=5.2$ Hz, 1H), 7.24~7.21 (m, 1H), 7.13~7.12 (m, 1H), 7.00~6.98 (d, $J=8.0$ Hz, 2H), 6.76~6.73 (d, $J=8.4$ Hz, 1H), 6.69~6.67 (d, $J=8.4$ Hz, 2H), 4.34~4.30 (d, $J=14.0$ Hz, 1H), 4.23~4.20 (d, $J=14.0$ Hz, 1H), 3.91~3.88 (m, 1H), 3.32~3.24 (m, 2H), 2.65~2.61 (t, $J=7.2$ Hz, 2H), 2.55~2.39 (m, 2H), 2.21~2.11 (m, 1H), 1.79~1.71 (m, 1H). $^{13}\text{C-NMR}$ (DMSO- d_6 , 150 MHz) δ : 170.21, 163.68, 156.15, 143.34, 131.08, 130.07 (2C), 129.65, 129.12, 125.70, 122.87, 115.51 (2C), 115.16, 64.53, 46.16, 44.79, 34.63, 30.11, 23.34. ESI-HRMS: calcd for $\text{C}_{20}\text{H}_{21}\text{BrN}_3\text{O}_2$, $[\text{M} + \text{H}]^+$, 414.0817, 416.0797; found 414.0817, 416.0795.

4.1.29.

(R)-*N*-(3-phenylpropyl)-1,2,3,9-tetrahydropyrrolo[2,1-*b*]quinazoline-1-carboxamide (**12i**)

Yield: 47.0%; $^1\text{H-NMR}$ (DMSO- d_6 , 600 MHz) δ : 8.32~830 (m, 1H), 7.30~7.27 (d, $J=7.2$ Hz 2H), 7.22~7.17 (m, 3H), 7.09~7.07 (m, 1H), 6.92~6.89 (m, 2H), 6.83~6.82 (d, $J=7.8$ Hz, 1H), 4.43~4.41 (d, $J=13.2$ Hz, 1H), 4.38~4.36 (d, $J=13.8$ Hz, 1H), 3.96~3.94 (m, 1H), 3.14~3.11 (m, 2H), 2.60~2.44 (m, 4H), 2.24~2.18 (m, 1H), 1.85~1.80 (m, 1H), 1.76~1.71 (m, 2H). $^{13}\text{C-NMR}$ (DMSO- d_6 , 150 MHz) δ : 170.54, 163.01, 143.83, 142.09, 128.78 (3C), 128.36, 126.55, 126.25, 123.87 (2C), 120.24, 64.58, 45.34, 38.70, 32.97, 31.31, 30.09, 24.47. ESI-HRMS: calcd for $\text{C}_{21}\text{H}_{24}\text{N}_3\text{O}_2$, $[\text{M} + \text{H}]^+$, 334.1919; found 334.1932.

4.1.30.

(R)-7-bromo-*N*-(3-phenylpropyl)-1,2,3,9-tetrahydropyrrolo[2,1-*b*]quinazoline-1-carboxamide (**12j**)

Yield: 46.9%; $^1\text{H-NMR}$ (DMSO- d_6 , 600 MHz) δ : 8.32~830 (m, 1H), 7.30~7.27 (t, $J=7.2$ Hz 2H), 7.24~7.16 (m, 5H), 6.76~6.75 (d, $J=8.4$ Hz, 1H), 4.43~4.41 (d, $J=13.8$ Hz, 1H), 4.38~4.35 (d, $J=14.4$ Hz, 1H), 3.97~3.95 (m, 1H), 3.14~3.10 (m, 2H), 2.60~2.46 (m, 4H), 2.25~2.19 (m, 1H), 1.85~1.79 (m, 1H), 1.76~1.71 (m, 2H).

^{13}C -NMR (DMSO- d_6 , 150 MHz) δ : 170.36, 163.73, 143.38, 142.09, 131.09, 129.17, 128.80 (2C), 128.78 (2C), 126.26, 125.72, 122.88, 115.14, 64.55, 44.85, 38.71, 32.97, 31.28, 30.16, 24.47. ESI-HRMS: calcd for $\text{C}_{21}\text{H}_{23}\text{BrN}_3\text{O}$, $[\text{M} + \text{H}]^+$, 412.1024; found 412.1034.

4.1.31.

(S)-*N*-((*S*)-1-hydroxy-3-phenylpropan-2-yl)-1,2,3,9-tetrahydropyrrolo[2,1-*b*]quinazoline-1-carboxamide (**13**)

Yield: 32.8%; ^1H -NMR (DMSO- d_6 , 400 MHz) δ : 8.15~8.13 (m, 1H), 7.32~7.21 (m, 5H), 7.08~7.04 (t, $J=7.2$ Hz, 1H), 6.93~6.89 (t, $J=7.2$ Hz, 1H), 6.80~6.78 (m, 2H), 4.89 (s, 1H), 4.11~4.04 (m, 2H), 3.86~3.84 (m, 1H), 3.74~3.70 (d, $J=13.6$ Hz, 1H), 3.44~3.34 (m, 2H), 2.94~2.90 (m, 1H), 2.64~2.58 (m, 1H), 2.51~2.37 (m, 2H), 2.15~2.07 (m, 1H), 1.79~1.74 (m, 1H). ^{13}C -NMR (DMSO- d_6 , 150 MHz) δ : 169.40, 162.22, 143.09, 138.99, 129.02 (3C), 127.89 (3C), 127.64, 125.78, 125.72, 123.17, 123.15, 119.45, 63.84, 63.00, 52.23, 44.23, 36.60, 29.45, 23.28. ESI-HRMS: calcd for $\text{C}_{21}\text{H}_{24}\text{N}_3\text{O}_2$, $[\text{M} + \text{H}]^+$, 350.1869; found 350.1863.

4.1.32.

(S)-*N*-(2-(1*H*-indol-3-yl)ethyl)-1,2,3,9-tetrahydropyrrolo[2,1-*b*]quinazoline-1-carboxamide (**14**)

Yield: 38.0%; ^1H -NMR (DMSO- d_6 , 400 MHz) δ : 10.83 (s, 1H), 8.33 (s, 1H), 7.56~7.54 (d, $J=7.6$ Hz, 1H), 7.35~7.33 (d, $J=8.0$ Hz, 1H), 7.16 (s, 1H), 7.08~7.04 (m, 2H), 7.00~6.96 (t, $J=7.6$ Hz, 1H), 6.92~6.85 (m, 2H), 6.82~6.80 (d, $J=7.6$ Hz, 1H), 4.31~4.20 (m, 2H), 3.92~3.89 (m, 1H), 3.45~3.40 (m, 2H), 2.89~2.85 (t, $J=6.4$ Hz, 2H), 2.55~2.44 (m, 2H), 2.21~2.14 (m, 1H), 1.82~1.75 (m, 1H). ^{13}C -NMR (DMSO- d_6 , 150 MHz) δ : 170.43, 162.99, 143.75, 136.70, 128.32, 127.75, 126.55, 123.84, 123.80, 123.26, 121.37, 120.25, 118.76, 118.69, 112.07, 111.84, 64.62, 45.23, 30.05, 25.51, 24.34. ESI-HRMS: calcd for $\text{C}_{20}\text{H}_{23}\text{N}_4\text{O}$, $[\text{M} + \text{H}]^+$, 359.1872; found 359.1871.

4.1.33. benzyl (*S*)-1,2,3,9-tetrahydropyrrolo[2,1-*b*]quinazoline-1-carboxylate (**16a**)

To a solution of **10a** (1.0g, 4.6 mmol) and triethylamine (1.3mL, 9.3 mmol) in anhydrous DMF (10 mL), BOP-Cl (1.4g, 5.5 mmol) was added at 0 °C, the mixture was stirred for 0.5 h at this temperature, then added benzyl alcohol (0.6mL, 5.8mmol),

and stirred for 5h at room temperature. 30mL H₂O was added to the resulting solution and stirred for 0.5 h, the solution was then extracted with ethyl acetate (20 mL × 3), the organic layers were combined and purified by flash chromatography on silica gel using ethyl acetate-petroleum ether (1:3 v/v) to give an oil, yield 38.2%. ¹H-NMR (DMSO-*d*₆, 600 MHz) δ: 7.42~7.38 (m, 5H), 7.17~7.15 (m, 1H), 7.03~7.00 (m, 2H), 6.90~6.89 (d, J=7.8 Hz, 1H), 5.22 (s, 2H), 4.62~4.60 (d, J=13.8 Hz, 1H), 4.58~4.56 (d, J=13.8 Hz, 1H), 4.42~4.40 (m, 1H), 2.71~2.60 (m, 2H), 2.43~2.36 (m, 1H), 2.07~2.02 (m, 1H). ¹³C-NMR (DMSO-*d*₆, 150 MHz) δ:171.02, 163.06, 136.05, 129.04, 129.02 (2C), 128.79, 128.60 (2C), 126.81, 124.99, 119.57, 67.08, 63.81, 45.56, 29.55, 23.82. ESI-HRMS: calcd for C₁₉H₁₉N₂O₂, [M + H]⁺, 307.1447; found 307.1449.

4.1.34. *4-methoxybenzyl*
(*S*)-1,2,3,9-tetrahydropyrrolo[2,1-*b*]quinazoline-1-carboxylate (**16b**)

Yield: 35.0%; ¹H-NMR (DMSO-*d*₆, 600 MHz) δ: 7.37~7.35 (m, 3H), 7.27~7.24 (m, 2H), 7.13~7.12 (d, J=7.8 Hz, 1H), 6.96~6.94 (m, 2H), 5.21~5.19 (d, J=12.0 Hz, 1H), 5.17~5.15 (d, J=12.0 Hz, 1H), 4.87~4.78 (m, 3H), 3.76 (s, 3H), 3.14~3.08 (m, 1H), 3.05~3.00 (m, 1H), 2.62~2.54 (m, 1H), 2.25~2.21 (m, 1H). ¹³C-NMR (DMSO-*d*₆, 150 MHz) δ:169.35, 164.91, 159.91, 130.74 (3C), 129.74, 127.72, 127.55, 127.45, 117.43, 114.39 (3C), 67.59, 65.67, 55.63, 45.68, 29.25, 23.70. ESI-HRMS: calcd for C₂₀H₂₁N₂O₂, [M + H]⁺, 337.1552; found 337.1562.

4.1.35. (*S*)-*N*-benzyl-1,2,3,9-tetrahydropyrrolo[2,1-*b*]quinazoline-1-carboximidamide (**20a**)

Thionyl chloride (30 mL) was added dropwise to a stirred solution of **10a** (8.0g, 37.0 mmol) in anhydrous ethanol (300 mL) at 0~5°C. Then the mixture was stirred at room temperature for 6 h and then concentrated under vacuum. The residue was alkalinized to pH 7~8 with a 5% aqueous solution of potassium carbonate and then extracted with ethyl acetate (50 mL × 3). After being washed with water and brine, the organic layers were dried over Na₂SO₄ and concentrated under reduced pressure to yield **17**. 100mL aqueous solution of ammonia (25%) was added, reacted at 50°C for 3h, the mixture was filtered and gave a white solid **18**, dried and added 30mL POCl₃, stirred at 50°C for 4h, cooled to room temperature, then the reaction solution was

poured into ice slowly, the mixture was alkalinized to pH 7~8 with a 10% aqueous solution of potassium carbonate and then extracted with ethyl acetate (40 mL × 3). The organic layers were combined and purified by flash chromatography on silica gel using ethyl acetate-petroleum ether (1:2 v/v) to give a white solid **19**. Dry HCl(g) was bubbled into an anhydrous ethyl alcohol solution of **19** (0.6g, 3.0mmol) for 0.5h, then the mixture was evaporated to dry under reduced pressure. Added 15 mL anhydrous ethyl alcohol and 5 mL Et₃N to the residue, stirred and phenylmethanamine (0.6mL, 5.5mmol) was added, stirred for 5 h at room temperature. Added 5 mL water and then the reaction solution extracted with ethyl acetate (40 mL × 3). The organic layers were combined and purified by flash chromatography on silica gel using ethyl acetate to give an oil, yield 35.1%. ¹H-NMR (DMSO-*d*₆, 400 MHz) δ: 9.56 (br, 2H), 7.47~7.33 (m, 5H), 7.14~7.01 (m, 1H), 7.01~6.98 (m, 2H), 6.92~6.90 (d, J=8.0 Hz, 1H), 4.61~4.52 (m, 2H), 4.45~4.42 (m, 2H), 4.36~4.32 (d, J=13.2 Hz, 1H), 2.66~2.58 (m, 2H), 2.53~2.44 (m, 1H), 1.96~1.87 (m, 1H). ¹³C-NMR (DMSO-*d*₆, 100 MHz) δ: 165.78, 163.98, 135.47, 129.48, 129.18 (3C), 128.47 (4C), 127.47, 127.06, 117.90, 64.60, 49.06, 46.08, 45.41, 29.63, 25.30. ESI-HRMS: calcd for C₁₉H₂₁N₄, [M + H]⁺, 305.1761; found 305.1758.

4.1.36.

(S)-N-(4-hydroxybenzyl)-1,2,3,9-tetrahydropyrrolo[2,1-b]quinazoline-1-carboximide (20b)

Yield: 37.3%; ¹H-NMR (DMSO-*d*₆, 400 MHz) δ: 9.67 (br, 3H), 7.21~7.19 (d, J=8.8 Hz, 2H), 7.15~7.11 (m, 1H), 7.00~6.95 (m, 2H), 6.91~6.89 (d, J=7.6 Hz, 1H), 6.80~6.78 (d, J=8.4 Hz, 2H), 4.50~4.39 (m, 4H), 4.32~4.28 (d, J=13.2 Hz, 1H), 2.63~2.59 (m, 2H), 2.51~2.41 (m, 1H), 1.92~1.83 (m, 1H). ¹³C-NMR (DMSO-*d*₆, 100 MHz) δ: 165.86, 163.02, 157.72, 129.76 (3C), 128.57, 126.59, 125.85, 124.65, 120.36, 115.83 (3C), 99.99, 63.01, 49.04, 45.45, 29.66, 25.41. ESI-HRMS: calcd for C₁₉H₂₁N₄O, [M + H]⁺, 321.1710; found 321.1708.

4.1.37.

(S)-N-(4-methoxybenzyl)-1,2,3,9-tetrahydropyrrolo[2,1-b]quinazoline-1-carboximide (20c)

Yield: 33.9%; $^1\text{H-NMR}$ ($\text{DMSO-}d_6$, 400 MHz) δ : 9.46 (br, 2H), 7.34~7.32 (d, $J=8.4$ Hz, 2H), 7.16~7.12 (m, 1H), 6.99~6.95 (m, 4H), 6.92~6.90 (d, $J=8.0$ Hz, 1H), 4.53~4.41 (m, 4H), 4.34~4.30 (d, $J=13.2$ Hz, 1H), 3.75 (s, 3H), 2.68~2.61 (m, 2H), 2.51~2.42 (m, 1H), 1.93~1.84 (m, 1H). $^{13}\text{C-NMR}$ ($\text{DMSO-}d_6$, 100 MHz) δ : 165.86, 163.13, 159.45, 129.82 (3C), 128.63, 127.66, 126.63, 124.77, 120.28, 114.51 (3C), 63.13, 55.64, 49.05, 45.29, 29.65, 25.46. ESI-HRMS: calcd for $\text{C}_{20}\text{H}_{23}\text{N}_4\text{O}$, $[\text{M} + \text{H}]^+$, 335.1866; found 335.1875.

4.2. Cell culture

SH-SY5Y cells were cultured in DMEM supplemented with 10% (v/v) fetal bovine serum (Hyclone). The cells were incubated in a humidified atmosphere of 5% CO_2 at 37 °C. All of the compounds were dissolved in dimethyl sulfoxide (DMSO) to 100 mM concentration and stored at -20 °C until the assay. DMSO was purchased from Amresco (Solon, OH, USA).

4.3. MTT assay

SH-SY5Y (1×5000) cells were seeded into 96-well culture plates in a final volume of 100 μL . The cells were grown for 24 h, then pretreated with different concentrations of target compounds (final concentrations: 0, 0.1, 1, 10, 100 μM) for 6 h. After these treatments, the medium was replaced with HEPES buffer (1 \times HMF, Mg^{2+} -free, CC0074, Leagene, China) with or without containing NMDA (2 mM) for 30 min. And then, HEPES buffer was replaced with fresh DMEM for another 12 h. At the end of indicated treatments, 3-(4,5-Dimethylthiazol-2-yl)-2,5-diphenyl-tetrazolium bromide (MTT, 0.5 mg/ml, M-2128, Sigma) was added to the medium and incubated for another 4 h at 37 °C, then the medium was replaced by 150 μL DMSO. The absorbance was measured at 490 nm with a microplate reader (ELX 800, Bio-TEK instruments, Inc.). Cell viability was expressed as a percentage with the control group as 100%. Ifenprodil (I2892, Sigma) was the control medicine.

4.4. Measurement of Intracellular Calcium Concentration

The concentration of intracellular calcium was measured with Fluo-3 AM (MA0195, meilunbio, China). SH-SY5Y cells were cultured in 3.5-cm plates at a

density of 8×10^4 cells/plate for 24 h, and then incubated with **5q** (10 μ M) for 3 h. After the treatment, the supernatant was removed and cells were incubated with Fluo-3 AM (5 μ M) for 30 min in the dark. Then, cells were washed twice with HEPES buffer. After these treatments, the cells were measured with a laser scanning confocal microscope (Leica). Prior to exposure to NMDA, the dye-loaded cells were scanned for 0.5 min to obtain the basal level of intracellular Ca^{2+} . Then, NMDA (finally concentration was 2 mM) was added to the cultures, and for the control group, an equal amount of HEPES buffer as the NMDA in model group was added. The images were recorded every 5 s with a laser scanning confocal microscope.

4.5. Western Blotting

SH-SY5Y cells were cultured and treated with different concentrations of **5q** (final concentrations: 0, 0.1, 1, 10 μ M) for 6 h, then the medium was replaced with HEPES buffer that with or without containing NMDA (2 mM) for 30 min. And then, HEPES buffer was replaced with fresh DMEM for another 4 h. After each treatment, SH-SY5Y cells were collected, total cellular proteins were extracted by RIPA (radio immunoprecipitation assay) lysis buffer, the protein concentration was determined by BCA assay. Equal amount of protein in each lysate sample was separated by SDS-PAGE (8% gel) under reducing conditions and then transferred to poly-vinylidene difluoride (PVDF) membranes (Millipore Corporation, Billerica, MA, USA). Total proteins were blocked with 5% non-fat milk and phosphorylation proteins were blocked with 5% BSA, which were dissolved in TBST (tris-buffered saline (TBS)-Tween 20) for 2 h at room temperature. Then membranes were incubated with specific primary antibodies including NR2B (Cell signaling technology, 4212S, USA), p-ERK1/2 (Cell signaling technology, 4370S, USA), and ERK1/2 (Cell signaling technology, 4695S, USA), α -tubulin (Proteintech Group, 66031-1-1g, USA), then shaking overnight at 4 °C. After three times of washing with TBST, the membranes were incubated with the anti-rabbit (H+L) HRP (horseradish peroxidase, Bioworld Technology, AB44171, USA) or anti-mouse IgG (H+L) HRP (Bioworld Technology, AB21172, USA) secondary antibody for 1 h at room temperature, followed by three times of washing with TBST. Membrane scanning was

performed using the ChemiDocTMXRS imaging system (Universal Hood II, Bio-Rad Laboratories), and then analyzed by ImageJ program (NIMH, Bethesda, MD, USA).

4.6. Computer Molecular Docking

The hit compound **5q** was imported to Discovery Studio (DS) 3.0, and the 3D conformations were generated by the “generate conformations” using the “best” conformation method. The crystal structure of NMDAR (PDB ID: 5EWJ) from RCSB Protein Data Bank (<http://www.pdb.org/>) was selected as the receptor. The binding site was defined by the co-complexed ligand (Ifenprodil) in the crystal structure and the docking protocols were set up on the default setting.

4.7. Metabolic Stability Study

10 μ L of compound (10 μ M) and 80 μ L of liver microsomes were mixture and incubated at 37 °C for 10 min, and then 10 μ L NADPH regenerating system was added. Samples were obtained at 0 min, 5 min, 10 min, 20 min, 30 min, and 60 min. respectively, and 300 μ L stop solution (cold in 4 °C, including 100 ng/mL tolbutamide and 100 ng/mL labetalol) was added to terminate the reaction. After oscillating for 10 min, the plates were centrifuged (3220 g) at room temperature for 20 minutes, and the supernatants were used for analysis.

Acknowledgments

We gratefully acknowledge the financial support from the National Natural Science Foundation of China (Grant 81502931), Fund for Career Development Support Plan for Young and Middle Aged Teachers in Shenyang Pharmaceutical University (Grant ZQN2015024), Student's Platform for Innovation and Entrepreneurship Training Program (Grant 201710163000175), Program for Innovative Research Team of the Ministry of Education, and Program for Liaoning Innovative Research Team in University.

Conflict of interest

The authors declare no any conflict of interest.

References

[1] B. Tewes, B. Frehland, D. Schepmann, D. Robaa, T. Uengwetwanit, F. Gaube, T. Winckler, W.

- Sipli, B. Wunsch, Enantiomerically Pure 2-Methyltetrahydro-3-benzazepin-1-ols Selectively Blocking GluN2B Subunit Containing N-Methyl-D-aspartate Receptors, *Journal of medicinal chemistry*, 58 (2015) 6293-6305.
- [2] M. Koller, S. Urwyler, Novel N-methyl-D-aspartate receptor antagonists: a review of compounds patented since 2006, *Expert opinion on therapeutic patents*, 20 (2010) 1683-1702.
- [3] M.E. Fundytus, Glutamate receptors and nociception: implications for the drug treatment of pain, *CNS drugs*, 15 (2001) 29-58.
- [4] P.C. Trippier, K. Jansen Labby, D.D. Hawker, J.J. Mataka, R.B. Silverman, Target- and mechanism-based therapeutics for neurodegenerative diseases: strength in numbers, *Journal of medicinal chemistry*, 56 (2013) 3121-3147.
- [5] G.E. Hardingham, H. Bading, The Yin and Yang of NMDA receptor signalling, *Trends in neurosciences*, 26 (2003) 81-89.
- [6] C. Taghibiglou, H.G. Martin, T.W. Lai, T. Cho, S. Prasad, L. Kojic, J. Lu, Y. Liu, E. Lo, S. Zhang, J.Z. Wu, Y.P. Li, Y.H. Wen, J.H. Imm, M.S. Cynader, Y.T. Wang, Role of NMDA receptor-dependent activation of SREBP1 in excitotoxic and ischemic neuronal injuries, *Nature medicine*, 15 (2009) 1399-1406.
- [7] A.R. Wild, E. Akyol, S.L. Brothwell, P. Kimkool, J.N. Skepper, A.J. Gibb, S. Jones, Memantine block depends on agonist presentation at the NMDA receptor in substantia nigra pars compacta dopamine neurones, *Neuropharmacology*, 73 (2013) 138-146.
- [8] A.J. Milnerwood, C.M. Gladding, M.A. Pouladi, A.M. Kaufman, R.M. Hines, J.D. Boyd, R.W. Ko, O.C. Vasuta, R.K. Graham, M.R. Hayden, T.H. Murphy, L.A. Raymond, Early increase in extrasynaptic NMDA receptor signaling and expression contributes to phenotype onset in Huntington's disease mice, *Neuron*, 65 (2010) 178-190.
- [9] J.M. Loftis, A. Janowsky, The N-methyl-D-aspartate receptor subunit NR2B: localization, functional properties, regulation, and clinical implications, *Pharmacology & therapeutics*, 97 (2003) 55-85.
- [10] H. Furukawa, S.K. Singh, R. Mancusso, E. Gouaux, Subunit arrangement and function in NMDA receptors, *Nature*, 438 (2005) 185-192.
- [11] J. von Engelhardt, I. Coserea, V. Pawlak, E.C. Fuchs, G. Kohr, P.H. Seeburg, H. Monyer, Excitotoxicity in vitro by NR2A- and NR2B-containing NMDA receptors, *Neuropharmacology*, 53 (2007) 10-17.
- [12] J.D. Sweatt, Mitogen-activated protein kinases in synaptic plasticity and memory, *Current opinion in neurobiology*, 14 (2004) 311-317.
- [13] G.M. Thomas, R.L. Huganir, MAPK cascade signalling and synaptic plasticity, *Nature reviews. Neuroscience*, 5 (2004) 173-183.
- [14] M.J. Kim, A.W. Dunah, Y.T. Wang, M. Sheng, Differential roles of NR2A- and NR2B-containing NMDA receptors in Ras-ERK signaling and AMPA receptor trafficking, *Neuron*, 46 (2005) 745-760.
- [15] S. Paul, J.A. Connor, NR2B-NMDA receptor-mediated increases in intracellular Ca²⁺ concentration regulate the tyrosine phosphatase, STEP, and ERK MAP kinase signaling, *Journal of neurochemistry*, 114 (2010) 1107-1118.
- [16] L. Mony, J.N. Kew, M.J. Gunthorpe, P. Paoletti, Allosteric modulators of NR2B-containing NMDA receptors: molecular mechanisms and therapeutic potential, *British journal of pharmacology*, 157 (2009) 1301-1317.

- [17] K. Williams, Ifenprodil, a novel NMDA receptor antagonist: site and mechanism of action, *Current drug targets*, 2 (2001) 285-298.
- [18] E. Falck, F. Begrow, E. Verspohl, B. Wunsch, Metabolism studies of ifenprodil, a potent GluN2B receptor antagonist, *Journal of pharmaceutical and biomedical analysis*, 88 (2014) 96-105.
- [19] B.L. Chenard, J. Bordner, T.W. Butler, L.K. Chambers, M.A. Collins, D.L. De Costa, M.F. Ducat, M.L. Dumont, C.B. Fox, E.E. Mena, et al., (1S,2S)-1-(4-hydroxyphenyl)-2-(4-hydroxy-4-phenylpiperidino)-1-propanol: a potent new neuroprotectant which blocks N-methyl-D-aspartate responses, *Journal of medicinal chemistry*, 38 (1995) 3138-3145.
- [20] R. Garner, S. Gopalakrishnan, J.A. McCauley, R.A. Bednar, S.L. Gaul, S.D. Mosser, L. Kiss, J.J. Lynch, S. Patel, C. Fandozzi, A. Lagrutta, R. Briscoe, N.J. Liverton, B.M. Paterson, J.J. Vornov, R. Mazhari, Preclinical pharmacology and pharmacokinetics of CERC-301, a GluN2B-selective N-methyl-D-aspartate receptor antagonist, *Pharmacology research & perspectives*, 3 (2015) e00198.
- [21] D. Stroebel, D.L. Buhl, J.D. Knafels, P.K. Chanda, M. Green, S. Sciabola, L. Mony, P. Paoletti, J. Pandit, A Novel Binding Mode Reveals Two Distinct Classes of NMDA Receptor GluN2B-selective Antagonists, *Molecular pharmacology*, 89 (2016) 541-551.
- [22] Y. Tian, C. Ma, L. Feng, L. Zhang, F. Hao, L. Pan, M. Cheng, Synthesis and biological evaluation of (–)-linarinic acid derivatives as neuroprotective agents against OGD-induced cell damage, *Archiv der Pharmazie*, 345 (2012) 423-430.
- [23] K. Szydłowska, M. Tymianski, Calcium, ischemia and excitotoxicity, *Cell calcium*, 47 (2010) 122-129.
- [24] G. Krapivinsky, L. Krapivinsky, Y. Manasian, A. Ivanov, R. Tyzio, C. Pellegrino, Y. Ben-Ari, D.E. Clapham, I. Medina, The NMDA receptor is coupled to the ERK pathway by a direct interaction between NR2B and RasGRF1, *Neuron*, 40 (2003) 775-784.
- [25] A. Sava, E. Formaggio, C. Carignani, F. Andreetta, E. Bettini, C. Griffante, NMDA-induced ERK signalling is mediated by NR2B subunit in rat cortical neurons and switches from positive to negative depending on stage of development, *Neuropharmacology*, 62 (2012) 925-932.

Highlights

- The mechanism details of **5q** were further investigated through three experiments.
- **5q** had key interactions with the both binding pockets of **1** and **4**.
- **5q** exhibited higher metabolic stability than ifenprodil.
- **5q** could be a lead for developing new and oral NR2B-selective NMDAR antagonists.